Eur. J. Mineral.
2002, **14**, 599-606

Lead-antimony sulfosalts from Tuscany (Italy). V. Definition and crystal structure of moëloite, $Pb_6Sb_6S_{14}(S_3)$, a new mineral from the Ceragiola marble quarry

PAOLO ORLANDI[1,*], ALAIN MEERSCHAUT[2], PIERRE PALVADEAU[2] and STEFANO MERLINO[1].

[1]Dipartimento di Scienze della Terra, Università di Pisa, Via S. Maria 53, I-56126 Pisa, Italy
[2]Laboratoire de Chimie des Solides, Institut des Matériaux J. Rouxel, UMR CNRS 6502,
2, rue de la Houssinière, 44 322 Nantes Cedex 3, France

Abstract: Moëloite is a new lead-antimony sulfosalt, $Pb_6Sb_6S_{14}(S_3)$, discovered in the Ceragiola marble quarry, near Seravezza town (Tuscany, Italy). Associated minerals are: sulphur, pyrite and enargite. It crystallizes as very thin needles and soft plumose aggregates of flexible thin fibres with a metallic lustre. Under the microscope it looks white, with moderate anisotropism, without polarization colours; reflectance values (air/oil): 40.0-37.8/26.6-24.2 (470 nm), 38.8-36.5/24.9-22.8 (546 nm), 38.6-36.7/23.4-21.4 (589 nm), 36.5-34.7/21.2-20.1 (650 nm). Moëloite is orthorhombic, space group $P2_122_1$, with unit cell parameters a 15.328(3), b 4.0400(8), c 23.054(5) Å; V 1427.6(5) Å^3, with $Z = 2$; $D_{calc.}$ 5.86 g/cm^3. Main X-ray powder diffraction lines [d(Å), I, *hkl*]: 3.724 (55)(106, 112), 3.427 (100) (403), 3.047 (85) (312, 214), 2.844 (58) (503), 2.779 (70) (016, 314), 2.753 (45) (116), 2.017 (80) (614, 020), 1.733 (50) ($01\underline{12}$, 618, $20\underline{13}$). The crystal structure reveals $Pb_6Sb_6S_{16}$ rods parallel to **b**, and connected along **c** by a $(S_3)^{2-}$ trimer due to an additional S atom, to form (100) rod-layers. The crystal structural formula is $Pb^{2+}_6\ Sb^{3+}_6\ S^{2-}_{14}\ (S_3)^{2-}$. The formation of moëloite is subordinated to a high sulfur fugacity, which explains the S excess of its formula. The name is in honour of Dr. Y. Moëlo (Nantes, France), who first synthesized this compound.

Key-words: moëloite, sulfosalt, lead, antimony, crystal structure, Tuscany, Italy.

Introduction

Sulfide ore deposits of Tuscany present a large variety of well crystallized lead sulfosalts, like meneghinite (Bechi, 1852) or geocronite. Recently, two new Pb-Sb species were found in the Buca della Vena iron deposit: scainiite (Orlandi *et al.*, 1999) and pillaite (Orlandi *et al.*, 2001), while a new Hg-Bi species, grumiplucite, was found in the Levigliani mercury mine (Orlandi *et al.*, 1998). A fourth one, moëloite, $Pb_6Sb_6S_{17}$, has been discovered in the Ceragiola marble quarry, near Seravezza town. Both the mineral and the mineral name have been approved in 1998 (CNMMN 98 – 045) by the Commission on New Minerals and Mineral Names of the International Mineralogical Association; the name is given in honour of Dr. Yves Moëlo, specialist of lead sulfosalt mineralogy, who also obtained and characterized the synthetic equivalent, Phase P, of this new mineral (Moëlo, 1983). The type material has been deposited at Museo di Storia Naturale e del Territorio, Università di Pisa (Via Roma 103, I-56011 Calci (PI), Italy).

A preliminary account of the new mineral and its properties, including the structural features, has been given on the occasion of the 31st International Geological Congress, Rio de Janeiro, August 6-17, 2000 (Orlandi *et al.*, 2000). The aim of the present paper is to give a detailed description of its occurrence, chemical composition, crystallographic properties and crystal structure.

1. Occurrence, paragenesis and geological setting

The small town of Seravezza is located in Versilia, at the southern rim of the mountain chain well known as Apuan Alps, a district in northern Tuscany (province of Lucca), about 35 km North of Pisa (Fig. 1). Seravezza quarrying area is located 20 km southwest of Carrara, the most famous marble deposit in Italy, where about 100 mineral species have been found up to now (Orlandi & Franzini, 1994).

Seravezza marbles crop at the southwestern rim of the tectonic window of the Apuan Alps. They are part of an epizonal metamorphic complex originating from a Tertiary Tuscan sedimentary sequence (Carmignani & Giglia, 1975). At Ceragiola, moëloite occurs within small cavities in the marble, and is associated with sulphur, pyrite and enargite. In those cavities many other sulfosalts have been found: guettardite (Bracci *et al.*, 1980), robinsonite (Franzini *et al.*,

---

*e-mail: orlandi@dst.unipi.it

0935-1221/02/0014-0599 $ 3.60

DOI: 10.1127/0935-1221/2002/0014-0599

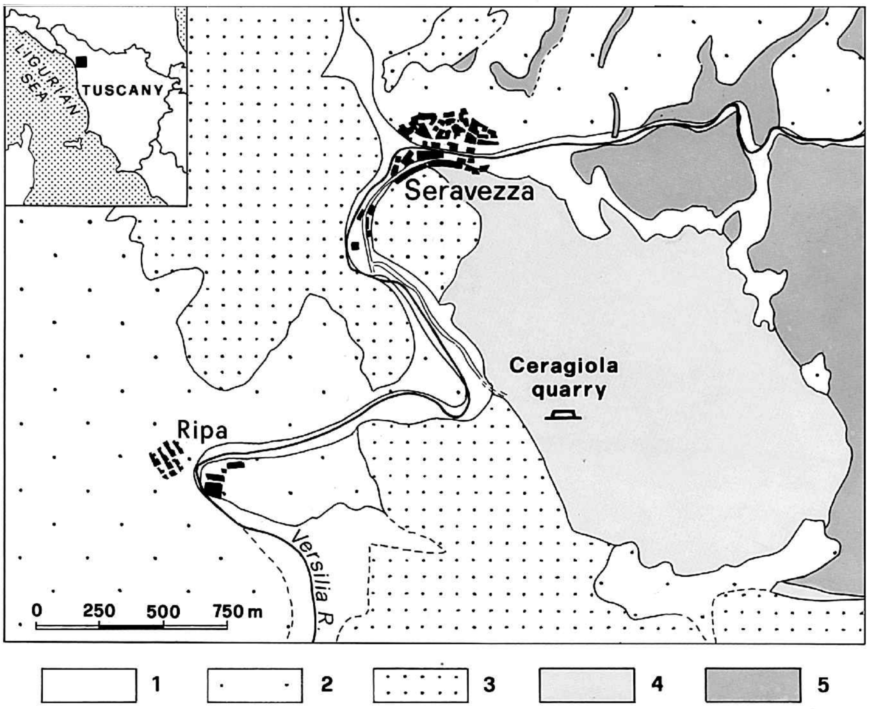

Fig. 1. Geographical location of the Ceragiola marble quarry, near Seravezza, with geological map of the area: 1. Alluvions, 2. Detritus and dumps. 3. Mid-triassic phyllites, metaconglomerates and quarzites 'Verrucano'. 4. Upper Triassic to Liassic carbonate platform deposits, mainly marbles. 5. Paleozoic basement. From Carmignani *et al.* (2000), simplified.

1992), zinkenite, boulangerite, semseyite, jordanite, tetrahedrite, together with sulvanite, colusite, famatinite and kësterite (Orlandi *et al.*, 1996).

2. Mineralogical characterization

2.1 Appearance and physical properties

Moëloite appears either as very thin needle-like [010] crystals (dimensions up to 0.1 x 0.1 x 5 mm), or as soft plumose aggregates of flexible thin fibres up to 5 millimeters long (Fig. 2). Moëloite exhibits a metallic luster and its colour varies from greyish-black to brownish-red for the finest fibres. The streak is brown. Under the microscope it is white, without pleochroism. Anisotropism is moderate, without polarization colours (like zinkenite); rare red internal reflections are visible in oil.

Table 1 gives the reflectance data obtained in air and oil on a randomly oriented crystal section for the two directions at 90° with minimum and maximum reflectivities. Reflectance values decrease regularly with increasing wavelengths (Fig. 3); bireflectance is weak, around 1-2 % in air and oil. Due to the small dimensions of the crystals, density and hardness could not be obtained. Calculated density resulted as 5.86 g/cm^3.

2.2 Chemistry

Table 2 gives the electron-probe micro-analytical data of moëloite, determined using an ARL-SEMQ-95 electron microprobe operating at 20 kV, with a specimen current of 20 nA and a beam spot size of 5 mm. No other element than Pb, Sb and S was detected.

The following standards and X-ray lines were used: PbS G-C for Pb and S (Pb$M\alpha$ and S$K\alpha$), Sb_2S_3 J-C-30 for Sb (Sb$L\alpha$). The raw data were corrected using the Magic-4 program (Colby, 1968).

The empirical structural formula, calculated on the basis of 17 sulfur atoms, is $Pb_{6.04}Sb_{6.06}S_{17}$, ideally $Pb_6Sb_6S_{17}$. Similar results were obtained by Moëlo (1983) in his study of the synthetic counterpart Phase P, as indicated by the comparison presented in Table 2. Considering the atomic ratios together with the normal valency states of Pb (+2), Sb (+3) and S (-2) in sulfides, it clearly appears a sulphur excess in the two analyses.

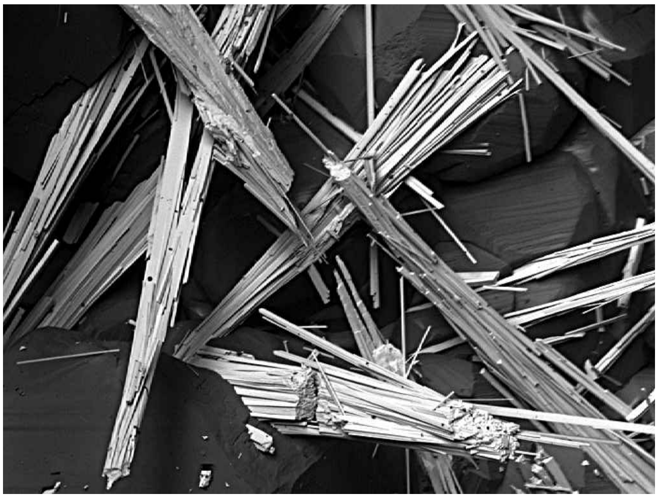

Fig. 2. SEM image of fibres of moëloite. The horizontal length of the photograph corresponds to 3 mm.

Table 1. Reflectance data (%) in air ($R1_{air}$ and $R2_{air}$) and oil ($R1_{oil}$ and $R2_{oil}$) on a random section of moëloite from Seravezza.

λ (nm)	$R1_{air}$	$R2_{air}$	$R1_{oil}$	$R2_{oil}$	λ (nm)	$R1_{air}$	$R2_{air}$	$R1_{oil}$	$R2_{oil}$	λ (nm)	$R1_{air}$	$R2_{air}$	$R1_{oil}$	$R2_{oil}$
400	40.0	37.0	29.3	26.7	***546***	*38.8*	*36.5*	*24.9*	*22.8*	680	34.6	33.6	20.2	19.6
420	40.7	38.8	27.8	25.7	560	38.5	36.8	24.4	22.2	700	33.2	32.1	19.8	18.8
440	40.8	39.2	27.6	25.3	580	38.7	36.5	23.7	21.6	720	33.0	32.2	19.2	18.1
460	40.0	37.7	27.1	24.6	***589***	*38.6*	*36.7*	*23.4*	*21.4*	740	33.1	31.3	18.3	17.7
470	*40.0*	*37.8*	*26.6*	*24.2*	600	38.1	36.4	23.3	21.4	760	31.3	29.6	17.6	17.0
480	40.0	38.2	26.6	24.3	620	36.9	34.5	22.2	21.0	780	30.8	29.4	18.0	16.9
500	40.1	38.2	25.9	23.6	640	36.1	34.5	21.6	20.2	800	30.8	27.5	17.7	17.0
520	39.5	37.8	25.4	23.4	***650***	*36.5*	*34.7*	*21.2*	*20.1*					
540	39.2	37.1	25.0	22.8	660	36.1	34.6	20.7	19.7					

Polishing method (on cloth): diamond; final buffing with Cr_2O_3. LEICA microscope with objectives FLUOTAR 20x/0.50 POL (air) and OEL 50x/0.85 (oil). Microscope photometer: Leica MPV-SP, monochromator: Δλ = 2 nm. Standard: SiC.

2.3 X-ray data

X-ray single crystal study indicated that moëloite is orthorhombic, space group $P2_12 2_1$. Unit cell parameters are: $a = 15.328(3)$, $b = 4.0400(8)$, $c = 23.054(5)$ Å; $V = 1427.6(5)$ Å^3, with $Z = 2$. The X-ray powder diffraction pattern of moëloite, collected with a Gandolfi camera, is reported in Table 3, together with that of its synthetic counterpart Phase P.

Table 2. Electron-probe micro-analysis of moëloite (mean of 4 spot analyses) and its synthetic counterpart (Phase P of Moëlo, 1983).

	Moëloite (*natural*)			**Phase P (*synth.*)**	
Element	wt.%	Range	Calc.	wt.%	Calc.
Pb	49.94	48.87-50.75	6.04	48.34	6.07
Sb	29.47	28.97-29.96	6.06	27.97	5.98
S	21.76	21.61-21.99	17.00	20.93	17.00
Total	101.17			97.24	

Calc.: calculated formula on the basis of 17 S atoms.

3. Crystal structure

3.1 Data collection

A very long needle-shaped crystal (0.01 x 0.01 x 0.7 mm), unfortunately slightly twisted, was mounted on a STOE image plate X-ray diffractometer. 215 images were recorded over the range 0° < φ < 215° with a φ–increment of 1°, after an exposure of 8 minutes for each φ position. The crystal-to-detector distance was set to 70 mm. Cell parameters were determined from a least-squares analysis of the setting angles of 5000 reflections in the range 5.3° < 2θ < 50.7°, which led to parameters $a = 15.328(3)$, $b = 4.0400(8)$, $c = 23.054(5)$ Å, $V = 1427.6(5)$ Å^3. The reflection intensities were recorded in the *hkl* range: $-18 < h < 18$, $-4 < k < 4$ and $0 < l < 28$. After the Lorentz-polarization correction of the 11512 collected (of which 5098 satisfied the criterion $F_0^2 > 4\,\sigma(F_0^2)$), equivalent reflections were averaged in the space group $P2_12 2_1$; this led to a set of 2693 independent reflections. Additional information about data collection as well as refinement conditions are given in Table 4.

The structure was solved by direct methods and subsequent difference Fourier calculations using SHELXTL programs (Sheldrick, 1996). The refinement carried on with anisotropic atomic displacement parameters for Pb and Sb and isotropic parameters for S, yielded a relatively high value $R_1 = 13.04$ %, with a goodness of fit S = 1.047, for 1329 reflections satisfying the criterion $F_0 > 4\,\sigma(F_0)$ and 89 parameters. Refinement carried on with anisotropic thermal parameters

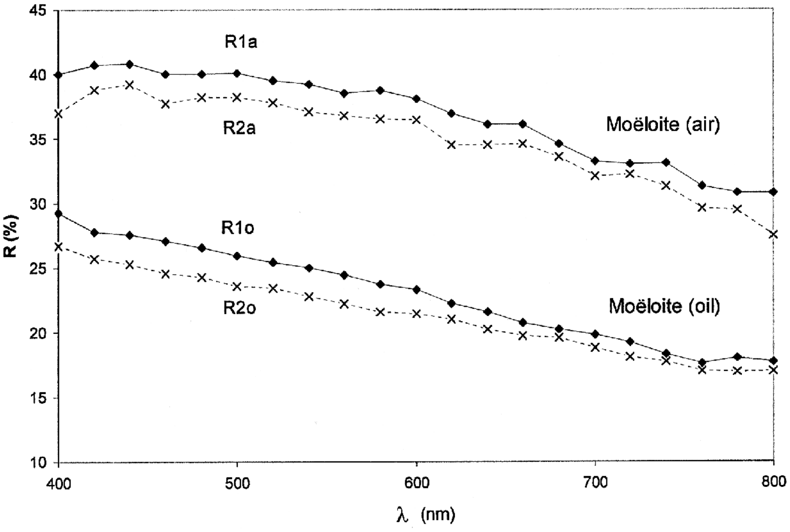

Fig. 3. Reflectance curves in air (R1a and R2a) and oil (R1o and R2o) for a random section of moëloite.

Table 3. X-ray powder diagram of moëloite and its synthetic equivalent Phase P.

Phase P		Moëloite						
I_{obs}	d_{meas}	I_{obs}	d_{meas}	d_{calc}	*h*	*k*	*l*	I_{calc}
				11.53	0	0	2	24
5	7.26	19	7.24	7.27	2	0	1	12
3	6.36	8	6.35	6.38	2	0	2	1
5	4.66	7	4.65	4.671	3	0	2	5
		< 1	4.421	4.415	1	0	5	3
22	4.25	19	4.248	4.255	3	0	3	25
		< 1	4.044	4.040	0	1	0	12
4	3.94	6	3.95	3.951	2	0	5	13
12	3.83	25	3.854	3.852	1	1	1	34
62	3.72	**55**	**3.724**	3.727	1	0	6	71
				3.700	1	1	2	14
		27	3.559	3.574	2	1	0	14
18	3.542			3.532	2	1	1	43
100	3.429	**100**	**3.427**	3.429	4	0	3	100
< 1	3.267	< 1	3.299					
10	3.216	18	3.232	3.241	2	1	3	9
				3.220	1	0	7	11
1	3.143	18	3.185	3.139	3	1	1	10
72	3.042	**85**	**3.047**	3.056	3	1	2	36
				3.037	2	1	4	56
15	2.977	17	2.952	2.981	1	1	5	23
				2.930	3	1	3	6
60	2.846	**58**	**2.844**	2.847	5	0	3	60
				2.825	2	1	5	13
90	2.774	**70**	**2.779**	2.784	0	1	6	42
				2.777	3	1	4	20
55	2.740	**45**	**2.753**	2.739	1	1	6	50
				2.707	5	0	4	13
				2.697	2	0	8	8
32	2.609	25	2.615	2.614	4	1	3	5
				2.612	3	1	5	18
1	2.497							
27	2.416	40	2.422	2.422	2	1	7	29
16	2.395	20	2.399	2.389	5	1	2	26
25	2.330	16	2.329	2.327	5	1	3	30
15	2.287	9	2.287	2.290	3	0	9	15
				2.284	3	1	7	6
18	2.241	9	2.240	2.243	2	1	8	16
		< 1	2.189	2.180	7	0	1	1
4	2.155	3	2.166	2.151	7	0	2	2
				2.150	6	1	1	4
2	2.125			2.130	4	0	9	4
40	2.095	28	2.096	2.101	3	0	10	16
				2.079	6	1	3	12
45	2.022	**80**	**2.017**	2.022	6	1	4	22
				2.020	0	2	0	32
7	1.965	4	1.964	1.966	5	0	9	6
				1.939	3	0	11	5
42	1.917	29	1.917	1.918	7	1	1	12
				1.916	8	0	0	14
				1.899	7	1	2	10
70	1.884	36	1.886	1.884	4	1	9	44
				1.864	2	0	12	5
< 1	1.844	3	1.829	1.825	3	2	3	9
9	1.807	11	1.808	1.809	6	0	9	4
				1.8079	2	1	11	4
				1.8057	6	1	7	5
6	1.778	6	1.784	1.7759	1	2	6	18
				1.7405	4	2	3	26
80	1.730	**50**	**1.733**	1.7350	0	1	12	14
				1.7280	6	1	8	8
				1.7277	2	0	13	8
				1.7146	8	0	6	5
24	1.653	25	1.655	1.6561	8	0	7	4
				1.6475	5	2	3	14
5	1.621	4	1.622	1.6188	5	2	4	5
4	1.580	4	1.581	1.5784	8	1	6	4
4	1.559	10	1.558	1.5570	9	0	6	8
5	1.515	5	1.517	1.5148	3	2	9	6
4	1.480	3	1.478	1.4777	7	1	10	4
				1.4612	3	1	14	4
40	1.456	27	1.458	1.4563	3	2	10	10
				1.4528	9	1	6	12
5	1.434	5	1.434	1.4331	10	1	0	5
				1.4303	10	1	1	6
				1.4178	7	1	11	3
5	1.413	3	1.415	1.4161	2	0	16	3
				1.4088	5	2	9	7
24	1.392	15	1.392	1.3901	8	2	0	11
				1.3829	3	1	15	6

Main observed lines in bold type. Indexation ($d_{calc.}$, *hkl*, $I_{calc.}$) on the basis of *a* 15.328, *b* 4.040 and *c* 23.054 Å. Weak lines with $I_{calc.} \leq 3$ have been omitted, except if no other line agreed with the observed ones.

also for S atoms did not significantly improve the *R* factor (R_1 = 12.82 % with 132 parameters); moreover seven among the nine S atoms had non positively defined values. The largest peak and hole in the difference map, *viz.* 12.2 and – 6.9 e-/ Å^3 respectively, as well as the lower peaks and holes, are found in the close neighborhood (about 1 – 1.1 Å) of each Pb atoms (Pb1, Pb2 and Pb3; Table 5): however, due to the relatively high background, even the largest peaks and holes are hardly significant. All these features, together with the high residual values, result from the very bad quality of the selected crystal and the consequent poor structure resolution. It is proper to remark that many attempts for absorption corrections did not improve the quality of the refinements. Thus, the set of uncorrected intensity data was retained, even though the too long needle dimension (**b** axis) implies that the observed intensities for (0*k*0) reflections are much greater than the calculated ones. Probably, the collection of well separated spots on different images was difficult because of overlap due to the twisting of the crystal along the needle axis. In fact a Weissenberg photograph *h*0*l* clearly showed the elongated shape of the spots due to the twisting effect. At this level of refinement, the structure solution is satisfying as regards the number of coordinated atoms with both Pb and Sb atoms, as well as values of their respective M-S distances (M = Pb or Sb).

3.2 Description of the crystal structure

Table 5 gives the atomic coordinates of the crystal structure, Table 6 the anisotropic displacement parameters for the cations, and Table 7 the metal-sulfur distances with corresponding bond valences. There are 15 independent atomic sites: 3 Pb, 3 Sb and 9 S. Fig. 4 gives the projection of the structure along **b**. The structure may be described, following the modular approach developed by Makovicky (1993, 1997), as based on lozenge-shaped rods derived from the SnS archetype; the rods, with $Pb_6Sb_6S_{16}$ composition, present accumulation of Sb atoms in rod interiors, whereas the large Pb cations are on the external parts of the rods, as clearly shown in Fig. 4. The rods are 3 Pb-polyhedra (3Q) large and the inner Sb atoms are arranged in such a way that their lone-electron pairs build up a ribbon-like micelle in the center of the rod. The peculiarity of the present structure-type lies in the way by which the apices of consecutive rods along **c** combine through an additional S9 atom, yielding a 'rod-layer' structure with composition $Pb_6Sb_6S_{17}$. The additional S9 atom builds up, through connection with two S5 atoms, a (S_3) trimer (Fig. 5); in this trimer the two equivalent S9-S5 distances are 2.03 Å long, this value is identical to the mean S-S distance within the S_8 group of elemental α sulfur

Table 4. Crystal structure of moëloite: Crystal data, data collection and refinement.

CRYSTAL DATA	
Structural formula	$Pb_6Sb_6S_{17}$
Formula weight	2518.73
Crystal system	orthorhombic
Space group	$P2_122_1$ (non conventional - n°18)
a	15.328(3) Å
b	4.0400(8) Å
c	23.054(5) Å
V	1427.6(5) Å^3
Z	2
Density (calculated)	5.86 g/cm^3
Absorption coefficient	42.05 mm^{-1}
DATA COLLECTION	
Temperature	293(2) K
Size of the crystal (mm)	0.01 x 0.01 x 0.7
Radiation	Mo $K\alpha$ (λ = 0.71073 Å)
Power	50 kV x 40 mA
Diffractometer	STOE IPDS single φ axis
Method	Imaging Plate Technology
φ range, $\Delta\varphi$ (increment)	0-215°, 1°
Crystal-to-detector distance (IP)	70 mm
Irradiation time per exposure	8 mn
θ range	2.65° to 25.73°
Independent reflections	2693 [R(int) = 0.1556]
Index ranges	$-18 \le h \le 18$, $-4 \le k \le 4$, $0 \le l \le 28$
REFINEMENT	
Refinement method	Full-matrix least-squares on F^2
Data/restraints/parameters	2693/0/89
Goodness-of-fit on F^2	1.047
final R indices [1329 reflections with I ≥ 2σ(I)]	R_1 = 0.1304
R indices (all data)	R_1 = 0.2071
Absolute structure parameter	0.44(7)
Largest diff. peak and hole	12.18 and -6.95 e.Å^{-3}

Table 5. Crystal structure of moëloite: Atomic coordinates (x 10^4) and equivalent isotropic displacement parameters (Å^2 x 10^3).

Atom	x	y	z	U(eq/iso)
Pb(1)	807(2)	0	1261(1)	29(1)
Pb(2)	1820(2)	-12(16)	2950(1)	22(1)
Pb(3)	3028(2)	-10(16)	4617(1)	21(1)
Sb(1)	1751(3)	5100(40)	6037(2)	63(2)
Sb(2)	645(3)	5110(40)	4304(2)	70(3)
Sb(3)	-605(4)	5400(30)	2563(3)	54(3)
S(1)	907(9)	4960(90)	2220(6)	15(3)
S(2)	2306(12)	-280(90)	6682(8)	31(5)
S(3)	2065(9)	5230(80)	3849(6)	15(3)
S(4)	3122(9)	5060(90)	5528(6)	15(3)
S(5)	-456(9)	4890(80)	699(6)	17(3)
S(6)	1216(11)	60(90)	5066(7)	30(4)
S(7)	173(10)	90(90)	3510(7)	25(4)
S(8)	-1015(13)	-340(90)	1885(8)	32(5)
S(9)	0	2380(80)	0	23(6)

U(eq) is defined as one third of the trace of the orthogonalized U^{ij} tensor.

Table 6. Anisotropic displacement parameters (in Å^2 x 10^3) for cations in the crystal structure of moëloite.

Atom	U_{11}	U_{22}	U_{33}	U_{23}	U_{13}	U_{12}
Pb(1)	51(2)	8(1)	28(1)	-1(3)	-3(1)	5(3)
Pb(2)	32(1)	11(1)	24(1)	2(2)	1(1)	0(3)
Pb(3)	24(1)	10(1)	29(1)	4(2)	-4(1)	1(3)
Sb(1)	18(3)	131(7)	39(3)	-17(8)	8(2)	-20(8)
Sb(2)	14(3)	168(9)	28(3)	19(7)	1(2)	-42(7)
Sb(3)	25(3)	76(7)	61(4)	53(5)	15(3)	9(5)

The anisotropic displacement factor exponent takes the form: $-2\pi^2[h^2a^{*2}U_{11} + ... + 2\ hka^*b^*\ U_{12}]$.

(Caron & Donohue, 1965), whereas the angle S5-S9-S5 (120°) is larger than the S-S-S angles in α sulfur (105°-109°). In moëloite, the S-trimer acts as a $(S_3)^{2-}$ group, and the crystal chemical formula becomes $Pb^{2+}{}_6\ Sb^{3+}{}_6\ S^{2-}{}_{14}\ (S_3)^{2-}$.

S-trimers form rows along **b**, and are connected to four Pb atoms having a triangular prismatic coordination [bicapped – Pb(3) , or tricapped – Pb(1); see Fig. 5]. As discussed beforewards, the connection of rods by these trimers builds up 'rod-layers' parallel to (100) (Fig. 6a). If the trimer is considered as a whole, the rod-layer corresponds to the type 5 of the classification by Makovicky (1993) of the fundamental rod-layer types; it can also be derived from type

Table 7. Crystal structure of moëloite: Interatomic distances around cations, with corresponding bond valences (B. V.) calculated according to Brese & O'Keeffe (1991).

	d (Å)	B. V.		d (Å)	B. V.		d (Å)	B. V.
Pb(1)-S(1)	2.988	0.31	**Pb(2)**-S(7)	2.836	0.46	**Pb(3)**-S(4)	2.898	0.39
-S(1')	3.010	0.29	-S(3)	2.852	0.44	-S(4')	2.937	0.35
-S(2)	3.053	0.26	-S(1)	2.971	0.32	-S(6)	2.964	0.33
-S(5)	3.054	0.26	-S(1')	2.986	0.31	-S(3)	3.002	0.29
-S(4)	3.088	0.23	-S(3')	2.987	0.31	-S(5)	3.113	0.22
-S(5')	3.113	0.22	-S(2)	3.218	0.16	-S(3')	3.130	0.21
-S(4')	3.119	0.21	-S(8)	3.343	0.12	-S(5')	3.195	0.17
-S(8)	3.144	0.20				-S(9)	3.291	0.13
-S(9)	3.302	0.13						
	Sum	**2.11**		**Sum**	**2.12**		**Sum**	**2.09**
Sb(1)-S(4)	2.407	1.12	**Sb(2)**-S(3)	2.417	1.09	**Sb(3)**-S(8)	2.408	1.12
-S(2)	2.533	0.80	-S(6)	2.802	0.39	-S(1)	2.455	0.99
-S(2')	2.767	0.42	-S(7)	2.815	0.37	-S(8')	2.866	0.32
-S(6)	3.114	0.17	-S(7')	2.826	0.36	-S(7)	3.127	0.16
-S(6')	3.135	0.16	-S(6')	2.831	0.36	-S(7')	3.285	0.10
	Sum	**2.67**		**Sum**	**2.57**		**Sum**	**2.69**

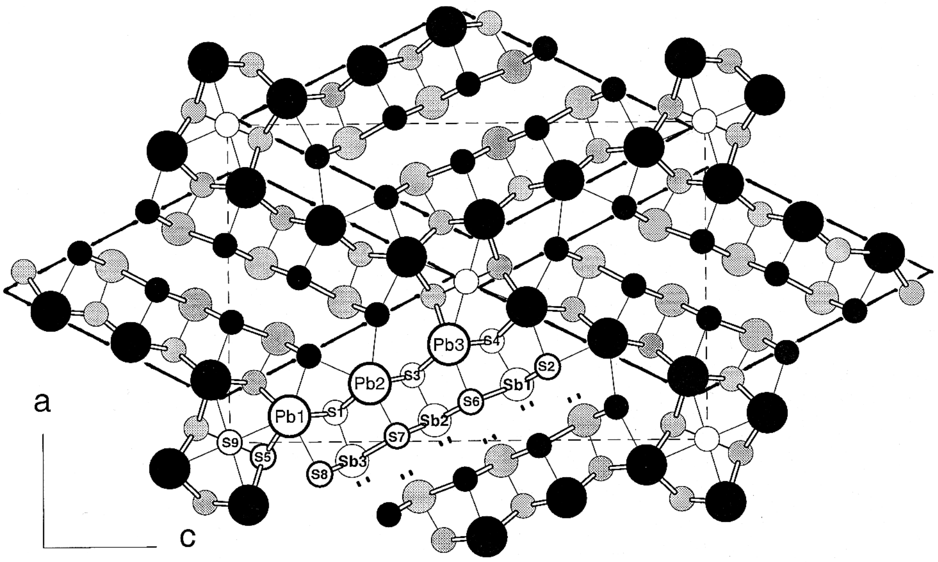

Fig. 4. Projection of the crystal structure of moëloite along **b**. Full black and grey circles indicate atoms with *y* close to 0 and 0.5, respectively; the open circles have y close to 0.25 (origin), or 0.75 (center). In the lower part double points close to Sb atoms represent their lone electron pair, forming a ribbon-type micelle along **b**. Thick lines indicate the lozenge section of $Pb_6Sb_6S_{16}$ rods parallel to **b**.

10 by insertion of an additional S atom (and changes due to a SnS-type, and not PbS-type, organization).

3.3 Related crystal structures

There exists a series of synthetic sulfides with a crystal structure very close to that of moëloite, but differing mainly by the lack of an additional S atom (Iordanidis *et al.*, 1999). One of the closest structures is presented by the compound $KLa_{1.28}Bi_{3.72}S_8$ (rod-unit formula: $K_2La_{2.56}Bi_{7.44}S_{16}$ - Fig. 6b). Without the additional S atom, the rod connection gives rise to the rod-layer type 5 (SnS archetype) of Makovicky (1993). Comparison of unit-cell parameters (Table 8) illustrates this similarity. As expected, the main relative change is observed for the *c* parameter, which corresponds to the direction of connection of rods.

Up to now, only one natural sulfosalt of the rod-layer type was known with a short S-S bonding; this mineral, livingstonite $HgSb_4S_6(S_2)$, shows a $(S_2)^{2-}$ pair in one of the two rod-layers constituting the crystal structure (Niizeki & Buerger, 1957; Fig. 6c). Among synthetic chalcogenides structurally related to the group of rod-layer sulfosalts, trimers of selenium atoms are known in $SrBiSe_3$ (Cook & Schäfer, 1982): here there are rods of the PbS archetype, 4Q large, with two $(Se_3)^{2-}$ trimers connecting two consecutive rods, giving the crystal structure formula $Sr_8Bi_8Se_{18}(Se_3)_2$ (Fig. 7). This compound can be considered as an expanded homologue of moëloite: the substraction in $Sr_8Bi_8Se_{18}(Se_3)_2$ of a sheared layer about two-atom-thick (2 Sr + 2 Bi + 4 Se + (Se_3) – open circles in Fig. 7) per rod-unit formula, gives the hypothetical moëloite pseudo-isotype (of the PbS archetype) $Sr_6Bi_6Se_{14}(Se_3)$. The comparison of unit-cell parameters (Table 8) illustrates this homologous relationship.

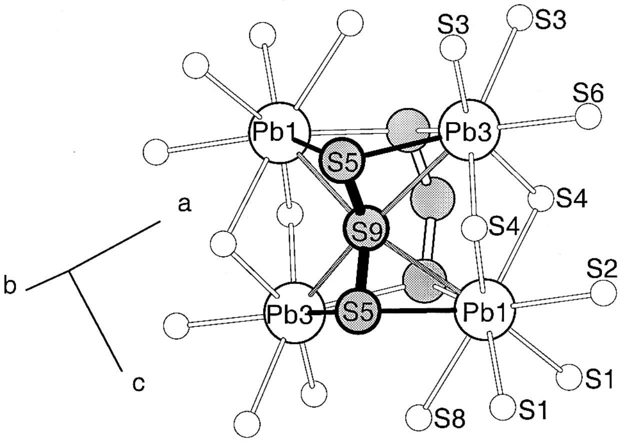

Fig. 5. Environment of the (S_3) trimer in the crystal structure of moëloite. Dark segments: strong bonds within the trimer (in front of the figure), and between this trimer and Pb atoms.

Recently, after our study had been completed, we became aware of a contribution by Choi & Kanatzidis (2000) presenting the structural arrangement of a novel polysulfide $Sr_6Sb_6S_{17}$. The structure is very similar to that of moëloite, as indicated by the corresponding unit cell parameters (Table 8) and differs from it, apart from the substitution of Sr for Pb (but with very similar Sr-S and Pb-S bond distances), in minor details: a) the translation periodicity along the elongation axis of the $Sr_6Sb_6S_{17}$ crystals (**a** axis, corresponding to the **b** axis in moëloite) is two times the corresponding value in moëloite; consequently the unit cell contains four formula units $Sr_6Sb_6S_{17}$, instead of two formula units $Pb_6Sb_6S_{17}$ as in moëloite; b) the trisulfide group presents a S-S-S bond angle of 113.8° and S-S distances of 2.09 Å, to compare with 120° and 2.03 Å, respectively, in moëloite; c) the coordination polyhedra around the six independent Sb cations in $Sr_6Sb_6S_{17}$ present, as it is normally found in Sb^{3+}, three short bonds (2.40 to 2.70 Å) and two longer bonds (3.0 to 3.4 Å) (Sb_{3+2}); in moëloite this occurs in two of the three independent Sb sites [Sb(1) and Sb(3)], whereas the coordination around Sb(2) is slightly different, with one short (2.42 Å) and four longer (2.80 to 2.83 Å) Sb-S bond distances (Sb_{1+4}) (Table 7).

This anomalous coordination, together with the U_{22} values, which appear high for all the Sb atoms, in particular

Fig. 6. *a.*

Fig. 6. *b.*

Fig. 6. *c.*

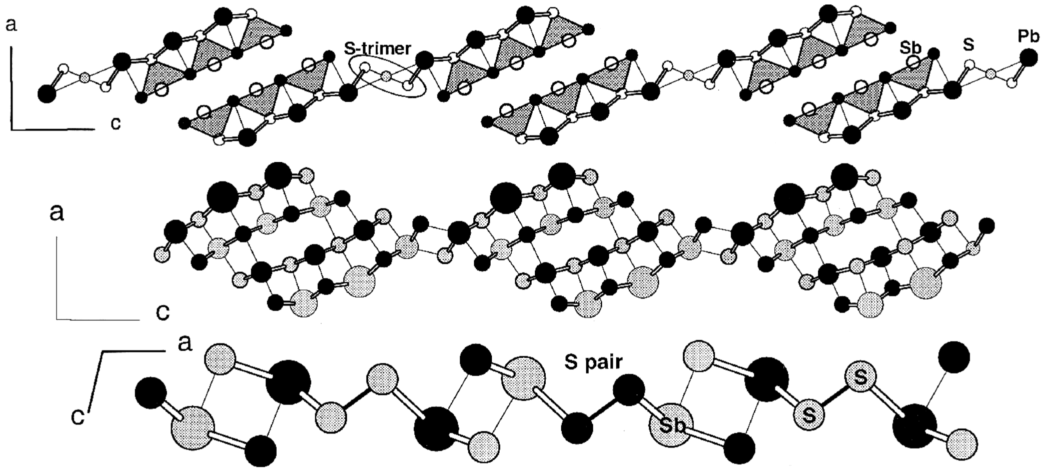

Fig. 6. *a.* The rod-layer of moëloite. Full and empty circles: *y* close to 0 and 0.5, respectively; grey circles: *y* close to 0.25. Grey triangles represent SbS_5 square pyramids. *b.* The rod-layer of synthetic $KLa_{1.28}Bi_{3.72}S_8$. In order of decreasing size circles denote K, (La,Bi), $(La_{\sim0.5},Bi_{\sim0.5})$, Bi and S. Full black and grey atoms have *y* equal to 0.25 and 0.75, respectively. *c.* One of the two constitutive rod-layers of livingstonite, with (S_2) pair; larger atoms are Sb. Full black and grey atoms have *y* close to 0 and 0.5, respectively.

for Sb(2) (Table 6), strongly suggested that the structural features of moëloite which we have presented actually correspond to the average structure, with a real structure demanding a doubling of the *b* parameter, as it occurs in $Sr_6Sb_6S_{17}$. As a matter of fact a long-exposure rotation photograph gave evidence of extremely weak and diffuse reflections actually corresponding to a trebling of the *b* parameter. The bad quality of the crystals at our disposal do not consent to go further in the structural study and to better define the finer details of the structural arrangement. However we retain that the main structural features of moëloite are already firmly established by the present study.

Table 8. Comparison of the unit cell data of moëloite and related synthetic compounds $KLa_{1.28}Bi_{3.72}S_8$, $SrBiSe_3$, $Sr_6Sb_6S_{17}$.

	Space group			
Moëloite	$P2_122_1$	*a* 15.328	*b* 4.0400	*c* 23.054 Å
$KLa_{1.28}Bi_{3.72}S_8$	*Pnma*	*a* 16.652	*b* 4.0712	*c* 21.589 Å
$SrBiSe_3$	$P2_12_12_1$	*b* 15.76	*b* 4.26	*c* 33.55 Å
$Sr_6Sb_6S_{17}$	$P2_12_12_1$	*b* 15.352	*a* 8.2871	*c* 22.873 Å

4. Conditions of formation of moëloite

At Seravezza, the scarcity and very irregular distribution of sulfides and related minerals (Orlandi *et al.*, 1996) does

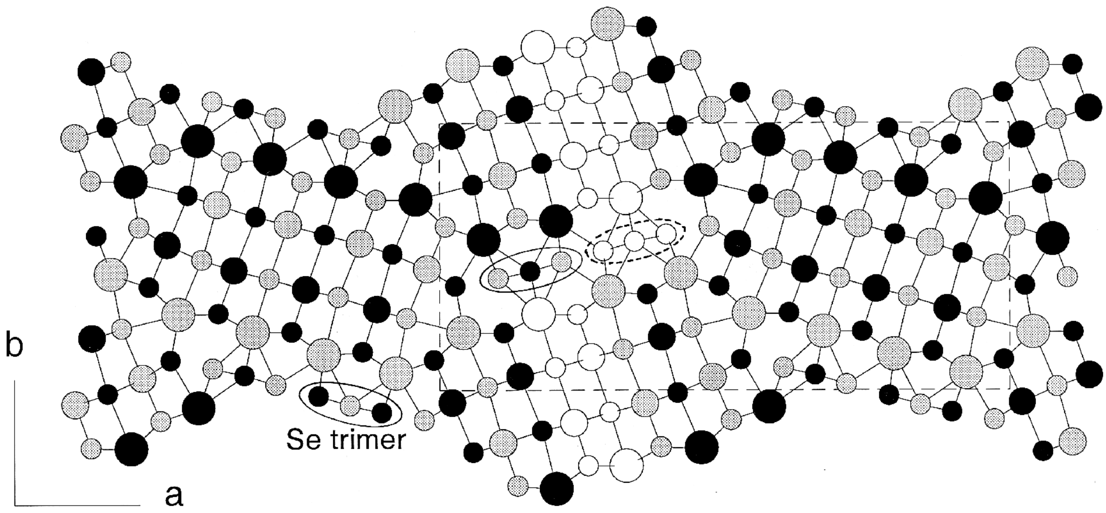

Fig. 7. The rod-layer of synthetic $SrBiSe_3$. In order of decreasing size circles denote Sr, Bi and Se. Full black and grey circles: *y* close to 0 and 0.5, respectively; open circles: atoms forming an additional sheared slab compared to moëloite structure. (Se_3) trimers form two adjacent columns parallel to **c**.

not allow to establish the general sequence of crystallization. One unique sample clearly shows the formation of very fine moëloite needles ("plumosite" texture) after well-crystallized robinsonite. Minerals indicating a high sulfur fugacity of the crystallization medium are: elemental sulfur (relatively frequent), enargite, luzonite and famatinite [high oxidation state (+5) of As and Sb, respectively], as well as the vanadium sulfides colusite and sulvanite.

According to the experimental data (Craig *et al.*, 1973), the formation of robinsonite indicates a relatively high temperature of formation (over 318°C). Phase P, the synthetic equivalent of moëloite, was obtained by dry way at 350 and 375°C, starting from crushed natural semseyite with a sulfur excess (Moëlo, 1983). From 400 to 430°C, a mixture of Phase P and boulangerite was obtained, while at 466°C and higher temperatures only boulangerite was observed. In the same conditions, natural boulangerite, chemically close to semseyite, did not yield any phase transformation. The minimum temperature of formation of Phase P is not known, due to the very slow reaction kinetic by dry way at low temperature, and, apparently, Phase P was never encountered in various studies by hydrothermal way (Moëlo, 1983). Nevertheless, the formation of Phase P is clearly related to a high sulfur fugacity fS_2, which explains the sulfur excess of its composition.

Without more accurate thermochemical data on the natural samples (for example, fluid inclusion studies), the temperature of formation of moëloite appears very imprecise, from above 300°C down to about 100°C or less. But it clearly appears that its formation is constrained by a very high sulfur fugacity, as it is also the case for the formation of livingstonite in Hg-Sb deposits (Craig, 1970).

Moëloite is the second natural sulfosalt with localized S-S bonding, the first being livingstonite, $HgSb_4S_6(S_2)$. One cannot exclude the existence of other natural phases with such S-S bonding.

Acknowledgements: We sincerely thank Dr. P. Léone (Institut des Matériaux J. Rouxel, Nantes), who kindly calculated the X-ray powder diagram from the crystal structure. The authors wish to thank L. Del Chiaro e S. Conforti who kindly gave us the first samples of moëloite for study, and P. Berlepsch and an anonymous referee for their useful indications.

P.O. and S.M. acknowledge the support by C. N. R., C. S. Geologia Strutturale e Dinamica dell'Appennino, Pisa.

References

Bechi, E. (1852): Intorno ad un nuovo minerale (meneghinite). *Atti Accademia Geogofili, Firenze*, **30**, 84.

Bracci, G., Dalena, D., Orlandi, P., Duchi, G., Vezzalini, G. (1980): Guettardite from Tuscany, Italy: a second occurrence. *Can. Mineral.*, **18**, 13-15.

Brese, N.E. & O'Keeffe, M. (1991): Bond-valence parameters for solids. *Acta Cryst.*, **B47**, 192-197.

Carmignani, L., Conti, P., Disperati, L., Fantozzi, P.P., Giglia, G., Meccheri, M. (2000): Carta geologica del Parco delle Alpi Apuane. S.E.L.C.A., Firenze.

Carmignani, L. & Giglia, G. (1975): Aperçu sur la géologie des Apuanes. *Bull. Soc. Géol. France*, sér.7, **17**, 963-978.

Caron, A. & Donohue, J. (1965): Bond lengths and thermal vibrations in orthorhombic sulfur. *Acta Cryst.*, **18**, 562-565.

Choi, K.S. & Kanatzidis, M.G. (2000): Sulfosalts with Alkaline Earth Metals. Centrosymmetric *vs* Acentric Interplay in $Ba_3Sb_{4.66}S_{10}$ and $Ba_{2.62}Pb_{1..38}Sb_4S_{10}$ Based on the Ba/Pb/Sb ratio. Phases Related to arsenosulfide Minerals of the Rathite Group and the Novel Polysulfide $Sr_6Sb_6S_{17}$. *Inorg. Chem.*, **39**, 5655-5662.

Colby, J.W. (1968): Quantitative microprobe analysis on thin insulating films. *Adv. X-Ray Anal.*, **11**, 287-305.

Cook, R. & Schäfer, H. (1982): Darstellung und Kristallstruktur von $SrBiSe_3$. *Rev. Chim. Minér.* **19**, 19-27.

Craig, J.R. (1970): Livingstonite, $HgSb_4S_8$: Synthesis and stability. *Am. Mineral.*, **55**, 919-924.

Craig, J.R., Chang, L.L.Y., Lee, W.R. (1973): Investigations in the Pb-Sb-S system. *Can. Mineral.*, **12**, 199-206.

Franzini, M., Orlandi, P., Pasero, M. (1992): Morphological, chemical and structural study of robinsonite ($Pb_4Sb_6S_{13}$) from Alpi Apuane, Italy. *Acta Vulcanologica, Marinelli Volume*, **2**, 231-235.

Iordanidis, L., Schindler, J.L., Kannewurf, C.R., Kanatzidis, M.G. (1999): $ALn_{1\pm x}Bi_{4\pm x}S_8$ (A = K, Rb; Ln = La, Ce, Pr, Nd): New semiconducting quaternary bismuth sulfides. *J. Solid State Chem.*, **143**, 151-162.

Makovicky, E. (1993): Rod-based sulphosalt structures derived from the SnS and PbS archetypes. *Eur. J. Mineral.*, **5**, 545-591.

— (1997): Modular crystal chemistry of sulphosalts and other complex sulphides. *In* Merlino, S. (ed.): *Modular aspects of minerals. EMU Notes in Mineralogy*, **1**, 237-271.

Moëlo, Y. (1983): Contribution à l'étude des conditions naturelles de formation des sulfures complexes d'antimoine et plomb. Signification métallogénique. B.R.G.M. ed., Orléans, Document **55**, 624 p.

Niizeki, N. & Buerger, M.J. (1957): The crystal structure of livingstonite, $HgSb_4S_8$. *Z. Kristallogr.*, **109**, 129-157.

Orlandi, P. & Franzini, M. (1994): I minerali del marmo di Carrara. Amilcare Pizzi S.p.a. Edit., 190 p.

Orlandi, P., Del Chiaro, L., Pagano, R. (1996): Minerals of the Seravezza marble, Tuscany, Italy. *Mineral. Record*, **27**, 47-58.

Orlandi, P., Dini, A., Olmi, F. (1998): Grumiplucite, a new mercury-bismuth sulfosalt species from the Levigliani mine, Apuan alps, Tuscany, Italy. *Can. Mineral.*, **36**, 1321-1326.

Orlandi, P., Moëlo, Y., Meerschaut, A., Palvadeau, P. (1999): Lead-antimony sulfosalts from Tuscany (Italy): I – Scainiite, $Pb_{14}Sb_{30}S_{54}O_5$, the first Pb-Sb oxy-sulfosalt, from Buca della Vena mine. *Eur. J. Mineral.*, **11**, 949-954.

Orlandi, P., Merlino, S., Meerschaut, A., Palvadeau, P. (2000): Moëloite, $Pb_6Sb_6S_{17}$, a new mineral from Tuscany, Italy. 31st Int. Geol. Congress, Rio de Janeiro, August 6-17, 2000, CD-ROM Abstracts Volume, Session 8-5.

Orlandi, P., Moëlo, Y., Meerschaut, A., Palvadeau, P. (2001): Lead-antimony sulfosalts from Tuscany (Italy): III – Pillaite, $Pb_9Sb_{10}S_{23}ClO_{0.5}$, a new Pb-Sb oxy-chloro-sulfosalt, from Buca della Vena mine. *Eur. J. Mineral.*, **13**, 605-610.

Sheldrick, G.M. (1996): SHELXTL Version 5. An integrated system for solving, refining and displaying crystal structures from diffraction data. Siemens Analytical X-ray Instruments Inc., Madison, Wisconsin (U.S.A.).

Received 8 May 2001
Modified version received 8 October 2001
Accepted 21 November 2001